U.S. DEPARTMENT OF COMMERCE
National Oceanic and Atmospheric Administration
Environmental Research Laboratories

NOAA Technical Memorandum ERL NSSL-65

RADIOSONDE ALTITUDE MEASUREMENT USING DOUBLE RADIOTHEODOLITE TECHNIQUES

Stephan P. Nelson

National Severe Storms Laboratory
Norman, Oklahoma
September 1973

TABLE OF CONTENTS

LIST OF FIGURES

LIST OF TABLES

RADIOSONDE ALTITUDE MEASUREMENT USING DOUBLE RADIOTHEODOLITE TECHNIQUES

Stephan P. Nelson
National Severe Storms Laboratory

The possibility of using double radiotheodolite methods to measure radiosonde altitude to within 15 m is investigated. Data were collected from a triad of stations with a 53.2 km average base line. Errors in computed balloon positions are an order of magnitude larger than expected from equipment accuracy considerations alone. The large height discrepancies are attributed to equipment alignment and ground reflection problems from viewing at low elevation angles over long base lines. Individual station biases were not ascertainable. Calculations determine optimum base-line lengths consistent with equipment accuracy, satisfactory viewing angles, and the desired 15 m altitude accuracy.

1. INTRODUCTION

Radiosonde altitude is conventionally derived from pressure via the hydrostatic approximation. Past soundings from the National Severe Storms Laboratory (NSSL) mesonetwork have used this same technique. However, when an instrument enters a severe thunderstorm, hydrostatic assumption is not always appropriate because high speed vertical drafts, entrainment, and water mass influence the vertical pressure distribution (Davies-Jones and Ward, 1971). Pressure distribution may greatly affect severe storm dynamics (Barnes, 1970). It is necessary to measure radiosonde heights within 15 m (about 1 mb at 500 mb) or less in order to determine these effects. Since the radiosonde signal can be detected from a station other than the launch station, even though separated by many kilometers, a double radiotheodolite method for measuring radiosonde altitude was studied.

2. BASIC DATA AND ANALYSIS

Experimental data were acquired from a triad of radiosonde stations (fig. 1) located in central Oklahoma at Norman (NRO), Mustang Airport (MAP) and Edmond (EDM) during NSSL's 1971 spring observation program. Two or all three stations tracked each instrument launched; table 1 lists the test cases. The sounding procedures are described by Barnes et al. (1971).

Table 1. List of Test Cases.

DAY (JUNE 71)	LAUNCH STATION	ASCENT NUMBER	TRACKING STATIONS	
7	MAP	37	NRO	EDM
8	MAP*	42	NRO	
8	EDM	41	NRO	
8	MAP	43	NRO	
10	MAP	44	NRO	
10	MAP	47	NRO	
10	EDM	44	MAP	EDM
10	NRO	50	MAP	
11	MAP	49	EDM	
12	MAP	50	NRO	

*Storm Environment

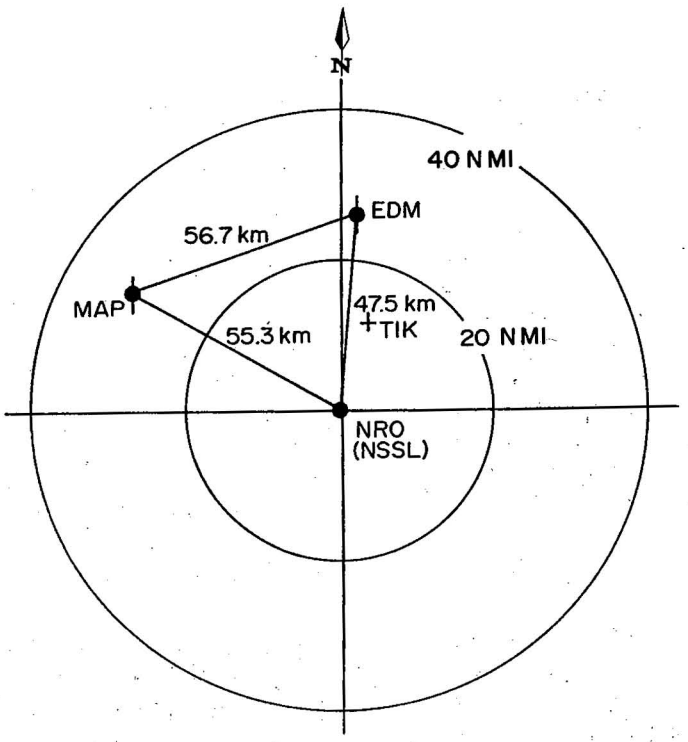

Figure 1. Location of test sites.

Two analysis techniques were employed to compute radiosonde height. The first method was developed by Thyer (1962). The second, a more common geometric method (for example, Middleton and Spilhaus, 1953), uses two azimuth angles to fix the horizontal position and either of the two elevation angles to fix the vertical position. Thyer bases his method on the fact that the two rays from the tracking antennas to the balloon almost never intersect in three-dimensional space due to error, instrument or human. However, a line connects the points of closest approach of the two rays. Thyer's method calculates the length of this line (termed the short line) and estimates the balloon's most probable position on this line. For our three-station configuration, the total length of any two rays is 50 to 100 km. If both azimuth and elevation angles are accurate to 0.1°, the expected short-line length (hence our uncertainty in positioning) is in the range of 40 to 80 m. However, we found that the computed short line distances exceed this calculated maximum error by an order of magnitude. Furthermore, balloon altitude calculated by the geometric method, using first one station's elevation angle and then the other's, reveals a discrepancy of several hundred meters. Clearly, the two tracking systems indicate the radiosonde is at two points in space several hundred meters apart.

Two possible sources of this error are explored: (1) inability to measure angles to the required resolution; (2) bias error due to alignment resulting from either mechanical or initial calibration problems. (Note: Elevation angle error may be azimuthally dependent if the tracking antenna is not absolutely level.) Both tracking systems (GMD-2 and WBRT-60) have azimuth (Az) and elevation (El) resolutions to hundredths of a degree. If these systems function to the manufacturer's specifications, limitations due to resolution should not be a factor in view of the above estimate of maximum short-line length for angle resolution 0.1°. Alignment is at least part of the problem because errors tended to be constant rather than random.

To study the error problem, we devised a test to determine whether any one station was at fault. Assume that one of a pair of stations viewing a balloon is tracking correctly and calculate the angles that the other station should be indicating. Comparing computed with measured values shows the nature of existing errors. The method uses the hydrostatic height computation in conjunction with the reference station's azimuth and elevation angles to determine balloon positions. Knowing length and orientation of the base line between the two tracking stations, we can calculate the angles that should have been measured from the second tracking station.

Data were divided into paired cases and the launch station data were used for height computations. Thus, the "reference system" changes as the launch station changes, complicating the analysis slightly. Only launch station data can be subjected to all necessary quality checks, since only one set of pre-flight

calibration data is available. There were six cases of the MAP-NRO pair (five MAP launches, one NRO launch), four cases of the MAP-EDM pair (three MAP launches, one EDM launch) and one case of the EDM-NRO pair (EDM launch). One sounding, MAP-NRO Asc 42, was taken in a severe thunderstorm, but height errors due to nonhydrostatic factors cannot account for the observed position discrepancies.

Actual values of the El and Az angles measured by the non-launch station were subtracted from the computed values:

1. δ_{El} = El [computed] - El [measured],

2. δ_{Az} = Az [computed] - Az [measured].

These delta values were plotted against time (figs. 2-12).

Notable features in figures 2 to 6 (MAP-NRO pair with MAP as the launch station) are positive delta values for El (heavy lines; means 0.05° to 0.50°) and larger negative values for Az (light lines, means -0.76° to -1.22°). When NRO is the launch station (fig. 7), there is no apparent change in the El delta values (mean 0.48°), but the Az delta values become positive (mean 0.27°). This sign change is likely to change in comparison standard as the launch station changes.

Some delta values appear fairly constant with time (fig. 2), whereas others fluctuate (fig. 7). The most unsteady portion of each data set generally occurs early in the sounding when the second tracking station's antenna is at a low elevation angle. One sounding (fig. 6) initially has a large delta value that soon diminishes. This may be due either to ground reflection or to the antenna not yet having locked into its target.

The MAP-EDM data (figs. 8-11) are similar to MAP-NRO. When MAP is the launch station (figs. 8, 9, 10), mean El and Az delta values range from 0.12 to 0.17° and -1.08 to -1.47°, respectively. When EDM launches, the Az delta values change to small positive (fig. 11), which is the same result observed in the MAP-NRO pair. For the only EDM-NRO case (fig. 12), the result is similar to the MAP-EDM and MAP-NRO tests and does not clarify the problem at all.

It would be helpful if we could isolate which station or stations are not indicating the correct Az and El angles. This is apparently impossible. If we assume only one station contains bias errors, then there must be no discrepancies between the other tracking station pair. The results (fig. 12) show that this is not a valid hypothesis. If only MAP had a bias error in azimuth, then since EDM and NRO deltas relate to MAP in the same manner, there should be no discrepancy between the EDM-NRO pair. But there is. Therefore, at least two stations have bias azimuth

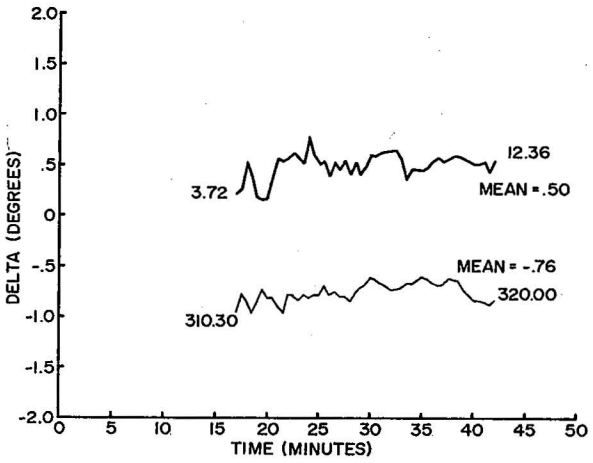

Figure 2. Delta El (heavy line) and Az (light line) values vs. time for MAP-NRO. The numbers at the ends are the values of the Az and El angles. MAP is the launch station. MAP ascent number 37.

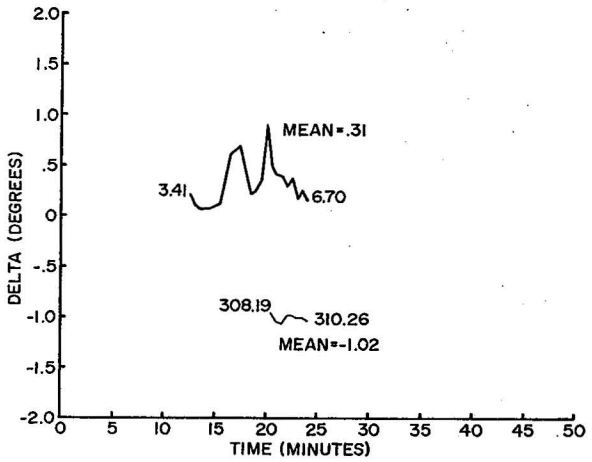

Figure 3. See figure 2. MAP ascent number 42.

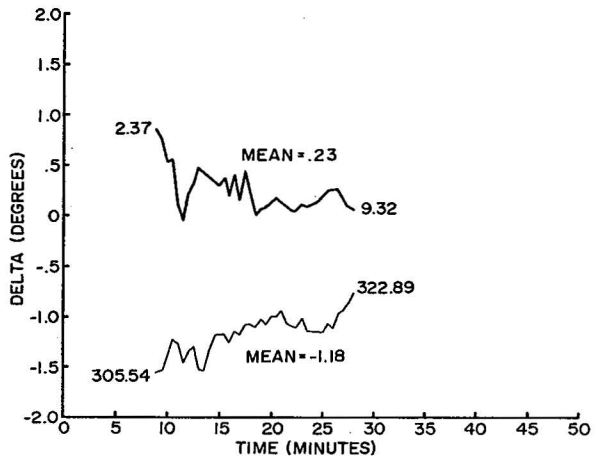

Figure 4. See figure 2. MAP ascent number 44.

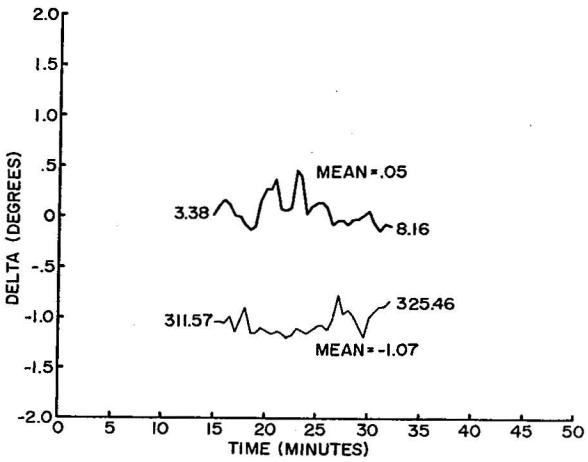

Figure 5. See figure 2. MAP ascent number 47.

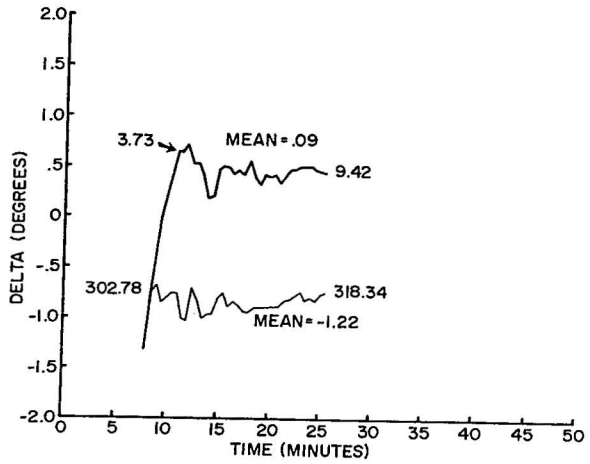

Figure 6. See figure 2. E1 mean is computed beginning at time 10.0. MAP ascent number 50.

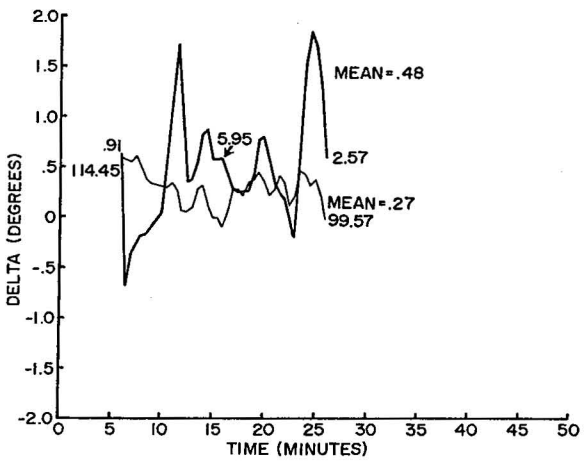

Figure 7. See figure 2. NRO is the launch station. NRO ascent number 50.

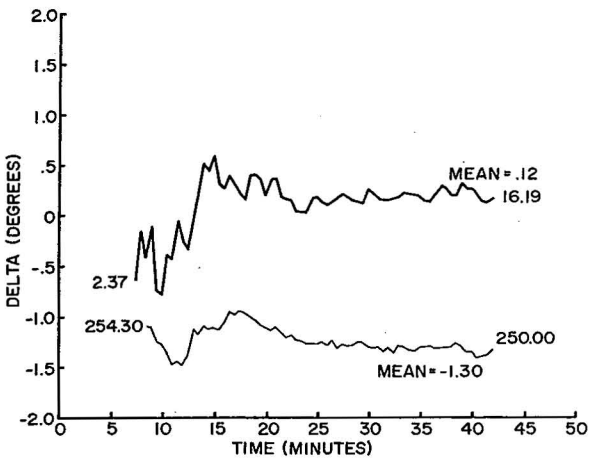

Figure 8. Delta E1 (heavy line) and Az (light line) values vs. time for MAP-EDM. The numbers at the end points are the values of the Az and E1 angles. MAP is the launch station. MAP ascent number 37.

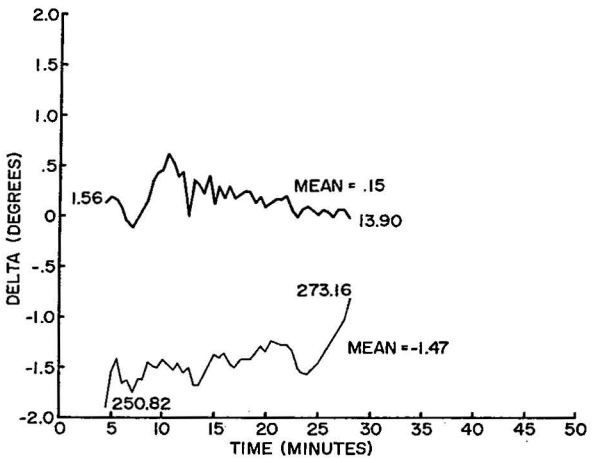

Figure 9. See figure 8. MAP ascent number 44.

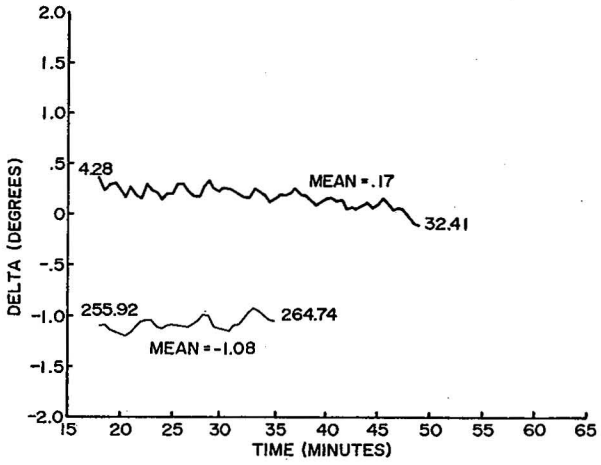

Figure 10. See figure 8. MAP ascent number 49.

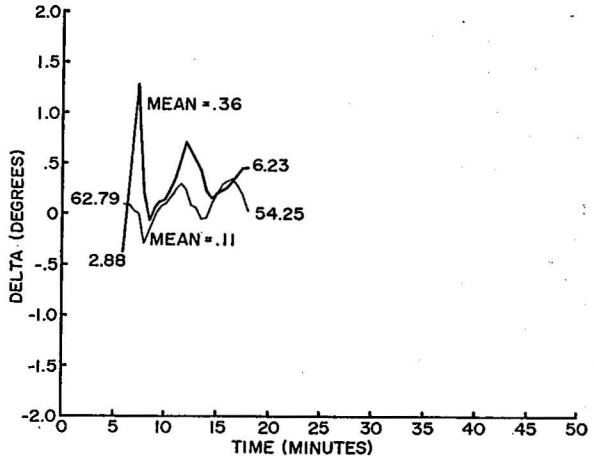

Figure 11. See figure 8. EDM is the launch station. EDM ascent number 44.

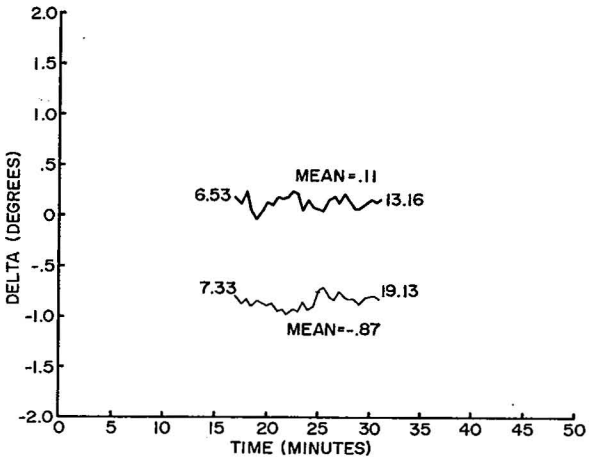

Figure 12. Delta El (heavy line) and Az (light line) values vs. time for EDM-NRO. The numbers at the end points are the values of the Az and El angles. EDM is the launch station. EDM ascent number 41.

errors and, with the available data, it is impossible to ascertain which two (or three) are wrong. A similar problem exists for the El angles.

If the error in El were azimuthally dependent, this would be evident through comparison of delta values separated in Az by 90°. The MAP-NRO data provide a test of this possibility. Figure 13 shows the net displacements of all dual tracked soundings between MAP and NRO. If a marked azimuthal error exists, it should be evident between the delta El values for the runs northeast of MAP and the one run northeast of NRO. The NRO-MAP El delta values (fig. 7) are not significantly different from the MAP-NRO runs. (Ignore the wild fluctuations caused by the extremely low elevation angle near the ends; the middle portions are comparable.) The mean NRO-MAP delta values is about 0.5° compared with 0.1 to 0.5° for MAP-NRO mean values. Apparently, no significant azimuthal dependency occurs in the El errors

MAP - NRO

DATE	ASC NO.	
6/7/71	37	A
6/8/71	42	B
6/10/71	44	C
6/10/71	47	D
6/12/71	50	E

NRO - MAP

6/10/71	50	F

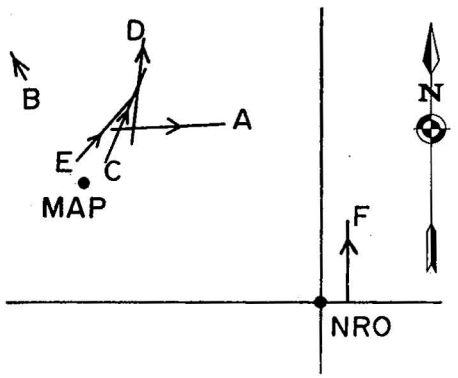

Figure 13. Net horizontal displacement of balloons during time of dual acquisition of signal; MAP-NRO.

This study has shortcomings. First, the data sample is small and doesn't cover a representative number of different flow situations. Antenna alignment errors are most easily recognized when soundings are accomplished under conditions where data are acquired in each quadrant. Also, the long base line between stations in this experiment (which was incidental to another experiment involving slant range data) require tracking at low elevation angles, which makes data accuracy questionable.

In summary, with the available data it does not appear possible to determine why the two instruments do not view the same point in space. Likely, much of the problem is caused by small, but ambiguous, antenna alignment errors and one station tracking at low elevation angles.

3. FUTURE WORK SUGGESTIONS

Two major factors must be corrected before we can obtain more accurate positioning data by double radiotheodolite: system accuracy and base line

distance. System errors consist of initial alignment and instrument limitations. The magnitude of the angle errors found in section 2 is not surprising. In the opinion of personnel who routinely operate radiotheodolites, the azimuth-elevation errors are between 0.5 and 1.0°. This is certainly sufficient for the intended purpose of the instruments, however, it is not adequate for the detailed measurements required in this study.

Errors might be reduced to acceptable limits by the following procedures. With the tracking antennas aligned as carefully as possible, comparative runs with one or two optical theodolites should be made. If after several tests a constant discrepancy appears, corrections can be applied to reduce this error. Then dual-tracked soundings (radiotheodolite) should be made in as many quadrants as winds will allow. The launch site should be alternated between the two stations. An independent check with a visual theodolite should be obtained from the launch site.

At the distances considered, the length of the short line ranges from 40 to 80 m even if both azimuth and elevation are accurate to 0.1°. If better accuracy is desired, the base line must be shortened. To see the relationship between base line length and instrument tolerance, we assume that hypothetical double radiotheodolite configuration in figure 14. Stations STA 1 and STA 2 are located on a north-south base line of length "b". Assume the balloon height above ground (Z) is 8 km and horizontal displacement (X) is 10 km due east of STA 1. For various base line values and different angle measurement uncertainties, we have listed the minimum short-line values in table 2. In general, position accuracy increases as base line decreases. For the stated conditions, positioning to about 20 to 25 m is possible only if angle errors are less than 0.1° and the base line is less than 10 km. Note that position accuracy doesn't increase significantly even though the base line is shortened from 10 to 1 km. Finally, a shorter base line minimizes earth curvature effects that complicate the tracking geometry between the two stations.

If stations are too far apart and the nonlaunch station views the balloon at low elevation angles, signal reflections produce considerable noise and cause erratic tracking. Considerable variability in the limiting elevation angle exists, but 6° above the horizon (or obstructions) seems to be a typical lower limit. Table 3 shows the elevation angle of the nonlaunch station for a variety of conditions. Relative balloon positions are indicated for ascents where the horizontal (X) to vertical displacement (Z) ratio is large (4.8) and small (1.2). Thus, Case 1 represents strong wind conditions and Case 2 is analogous to a light wind situation. The table shows results for three base line distances: 50, 10, and 1 km. For a 50-km base line, the probe must rise to at least 5 km altitude before the nonlaunch station El angle becomes greater than 6°. With a 10-km

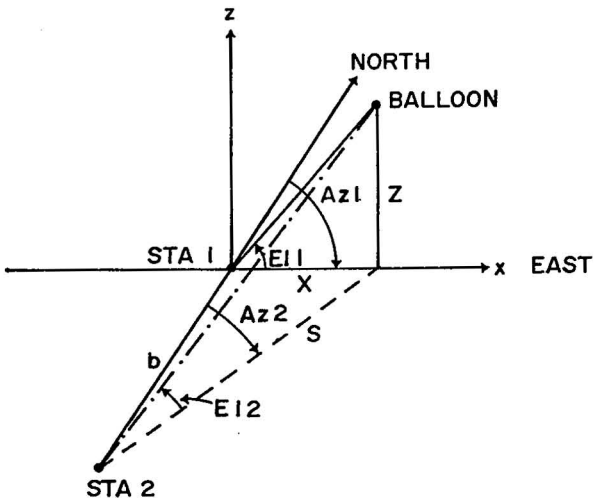

Figure 14. Hypothetical double radiotheodolite configuration.

Table 2. Minimum Short-Line Values in Meters as a Function of Base-Line Length (b) and Absolute Error in Az/El Angles.

	Absolute Az/El Angle Accuracy [DEG]				
	0.01	0.1	0.2	0.5	1.0
b = 50 km	5.6	56.2	112.4	281.1	562.2
b = 25 km	3.6	35.7	71.4	178.4	356.9
b = 10 km	2.5	25.4	50.7	126.8	253.5
b = 5 km	2.3	23.2	46.3	115.9	231.7
b = 1 km	2.2	22.4	44.8	111.9	223.8

Table 3. Viewing Angle Above Horizon of Nonlaunch Station (E12) for Different Base Lines (b). Cases 1 and 2 Represent Strong and Light Wind Conditions, Respectively.

Case 1: X/Z = 4.8				Case 2: X/Z = 1.2			
X(km)	Z(km)	S(km)	E12(DEG)	X(km)	Z(km)	S(km)	E12(DEG)
			b = 50 km				
3.39	1.30	50.12	1.5	0.50	3.40	50.00	3.9
8.16	2.35	50.67	2.7	3.57	4.93	50.13	5.6
14.07	3.45	51.94	3.8	7.66	6.42	50.58	7.2
20.36	4.63	53.99	4.9	9.42	8.13	50.88	9.1
27.87	5.83	57.24	5.8	11.33	9.70	51.27	10.7
			b = 10 km				
3.39	1.30	10.56	7.0	0.50	3.40	10.01	18.7
8.16	2.35	12.91	10.3	3.57	4.93	10.62	24.9
14.07	3.45	17.26	11.3	7.66	6.42	12.60	27.01
20.36	4.63	22.68	11.5	9.42	8.13	13.74	30.6
27.87	5.83	29.61	11.1	11.33	9.70	15.11	32.7
			b = 1 km				
3.39	1.30	3.53	20.2	0.50	3.40	1.12	71.8
8.16	2.35	8.22	16.0	3.57	4.93	3.71	53.0
14.07	3.45	14.11	13.7	7.66	6.42	7.73	39.7
20.36	4.63	20.39	12.8	9.42	8.13	9.47	40.6
27.87	5.83	27.89	11.8	11.33	9.70	11.37	40.5

base line, the 6° limit is passed before the balloon reaches 1.3 km altitude--in most cases near cloud base for severe thunderstorms in Oklahoma. Base lines of 1 km over-compensate for the low elevation angle problem and cause another problem in which the accuracy of the height measurement deteriorates as the balloon gets higher because the two antennas view along nearly the same path.

If sufficient alignment and maintenance procedures are performed, the double radiotheodolite method may be capable of positioning the balloon's altitude within 20 to 25 m, provided the tracking stations are no further than 10 to 20 km apart.

4. ACKNOWLEDGMENTS

The author thanks members of the NSSL staff and especially Dr. Stanley L. Barnes for helpful conversations and review of the paper.

5. REFERENCES

Barnes, S. L., 1970: Some aspects of a severe, right-moving thunderstorm deduced from mesonetwork rawinsonde observations. J. Atmos. Sci., 27, 634-648.

_____, J. H. Henderson and R. J. Ketchum, 1971: Rawinsonde observation and processing techniques at the National Severe Storms Laboratory. NOAA Technical Memorandum ERL NSSL-53, National Severe Storms Laboratory, Norman, Oklahoma, 246 pp.

Davies-Jones, R. P., and N. B. Ward, 1971: Comments on some aspects of a severe right-moving thunderstorm deduced from mesonetwork rawinsonde observations. J. Atmos. Sci., 28, 652-653.

Middleton, W. E. and A. F. Spilhaus, 1953: Meteorological Instruments. Toronto, University of Toronto Press, 286 pp.

Thyer, N., 1962: Double theodolite pibal evaluation by computer. J. Appl. Meteor., 1, 66-68.

APPENDIX

RADIOSONDE ALTITUDE MEASUREMENT USING SLANT RANGE

A.1 INTRODUCTION

An alternate method to determine radiosonde altitude from measured slant range and elevation angle was studied in the Spring of 1971. Data were collected from the same three sites used for the double theodolite study--Edmond, Mustang Airport, and Norman (see fig. 1). Each tracking antenna (two GMD-2's, one WBRT-60) was capable of measuring the slant range to a VIZ 1199* radio transponder. The limitations of altitude derivation using slant range are examined.

A.2 ANALYSIS

Raw slant range data were used in conjunction with antenna elevation angles to compute the height above the surface (corrected for earth's curvature) at half-minute intervals. Hydrostatic heights (PHEIGHT), which are assumed to be correct, were compared with slant range heights (SRHT).

DELTA = PHEIGHT - SRHT

Table A.1 shows the mean of the absolute delta values (MAD) for all transponder soundings from the three stations. It was hoped that the delta values would be of the same order as the RMS errors of the ranging system (approximately 5 to 25 meters at the operating distances). However, the results in general are disappointing. MAD values ranged from 19.5 to 1,002.9 m, while the lowest average for any station's ensemble of soundings was 81.1 m. To determine if the source of errors could be isolated and corrected, the delta values were plotted against time for each sounding. Each station was found to have a distinct dominant delta versus time signature (hereafter called error signature). For this reason the results are discussed individually by station.

A.2.1 Edmond (EDM, GMD-2)

Of the three stations, EDM exhibited the best initial results. In the main two basic error signatures surface (figs. A.1 and A.2). The first error is characterized by deltas,

*Citing trade names and manufacture's names in this report is not to be construed as official government endorsement or approval of commercial products or services referenced herein.

never very large, oscillating about zero. The mean and MAD are 6.5 and 23.8 m. This sounding is within the tolerances of height measurements expected. In figure A.2 the deltas behaved well up to a point in time after which the errors grow quite quickly producing a slope discontinuity. Eight of EDM's 26 soundings exhibited this discontinuity. A comparison between MAD before this break point and the MAD for the entire sounding (table A.2) showed an average improvement of 115.5 m per run. This lowered EDM's overall average to 45.0 m.

An attempt was made to determine whether the break point of each case is predictable. Figure A.3 is a scattergram of elevation angle and slant range distances. The specific slant ranges and elevation angles plotted are for: (1) the break point if the case exhibited the discontinuity (*), and (2) the last point of the run for the remaining cases (·). The ascent number of each case is indicated. Three of the cases (ascent numbers 38, 41, and 44) suffered balloon breaks, and due to the resultant erratic tracking, are not considered comparable to the others. Of the ten cases with slant range greater than 30 km and elevation angles less than 15°, seven produced the error signature. Only one case with the signature was outside this range.

Three corrections are common to all stations' data: (1) compensation for atmospheric ray refraction (4/3 R correction where R is mean earth radius), (2) slant range correction, and (3) elevation angle correction. The 4/3 R correction improved 17 of the EDM runs by an 4.2 m average and worsened nine cases by a 3.4 m average. This is of minimal value.

The slant range and elevation angle corrections use the same basic approach. For slant range the elevation angle and PHEIGHT are assumed correct, and the slant range is calculated. If a constant bias is present between computed and measured values, then measured values can be corrected by the constant amount. The elevation angles can be corrected in a similar manner on assuming slant range and PHEIGHT are correct. However, for EDM neither slant range nor elevation corrections were consistent enough to warrant application.

In summary, the EDM slant range computed heights agree with the hydrostatically computed heights within a 45 m average if one acknowledges the 30 km slant range and 15° elevation limitations.

A.2.2 Mustang Airport (MAP, GMD-2)

The MAP mean absolute deltas were considerably poorer than EDM. An example of the MAP dominant error signature is shown in figure A.4 (ascent number 31). Generally errors were initially small, but increased steadily with time. The average disagreement between PHEIGHT and SRHT was 135.2 m. The 4/3 R correction increased errors in 23 cases and decreased them in only two cases.

In checking for an elevation correction, a constant discrepancy of approximately 0.35° appeared. This correction was applied to all cases and the SRHT's recomputed. Figure A.5 shows this correction's effect on ascent number 31 (fig. A.4). The MAD improved from 120.6 to 27.5 m. Overall, 20 soundings improved by 62.5 m and five deteriorated by 53.0 m on average. This caused the average MAD for all MAP soundings to decrease from 135.2 to 95.8.

A.2.3 Norman (NRO, WBRT-60)

Norman yielded the worse results with an average error of 183.9 m. As with the other two stations, the 4/3 R correction was of little value. Unsteadiness characterized the NRO runs. A.6 shows one type of error signature that was easy to correct. The step discontinuity is due to the slant range changing drastically between two half-minute periods--probably attributable to a tracking instrument malfunction. This error type is easily detected and is corrected by ignoring all points after the jump. In principle the incorrect points could be adjusted to follow the prejump trend. However, this problem should be corrected at the instrument level and normally would not appear in the data. These corrections improved five cases by an average of 419 m.

Six NRO cases exhibited the same delta discontinuities as eight of the EDM cases (e.g., fig. A.2). Corrected in the same manner as for EDM, the NRO cases improved an average of 91.4 m. Interestingly, at the break points, four of six cases have slant ranges larger than 30 km and elevation angles less than 15°. This suggests the same type signal evaluation problems at low elevation angles with large ranges that are common to radio tracking systems.

For NRO soundings all the corrections combined lowered the MAD from 183.9 to 111.9 m.

A.3 SUMMARY

Each station suffered from errors that were in the main distinct. The average absolute differences between the SRHT and PHEIGHT were 81.1, 135.2, and 183.9 m for EDM, MAP, and NRO. In eight EDM cases, errors were reduced by an average of 115.5 m by ignoring all points after a discontinuity in the slope of a plot of deltas versus time. This caused the overall average of EDM to decrease to 45 m. In attempting to isolate the cause of error, it was found that the data should be omitted if the elevation angle is less than 15° and the slant range larger than 30 km.

MAP appeared to suffer from a 0.35° elevation angle error. This correction caused the average absolute error to decrease from 135.2 to 95.8 m.

NRO was the most unsteady of the three stations. Some errors were easy to identify and were corrected by ignoring all points past the range jump. Six cases resembled the error signature experienced by EDM and accordingly were corrected. All combined adjustments reduced the absolute error by 72 m to 111.9 m.

Weiss (1969) in a similar study found the average of the mean absolute differences between the SRHT's and heights determined by radar was 231 m. The errors in this study are less. The smaller errors are probably due to the corrections applied; moreover, errors tend to increase with slant range and Weiss' flights were longer and presumably the radiosondes drifted farther from the tracking antenna.

Even the best results show that the tested slant range procedure for determining radiosonde altitude is too gross for detailed severe storm research. This method is especially unsuitable due to possible data loss in applying various corrections.

REFERENCES

Weiss, Bernard D., and E. J. Georgian, 1969: Test Report: AN/GMD-2A Rawin Set-AN/FPS-16 Radar Comparison, Air Force Cambridge Research Lab., Instrumentation Papers, No. 162, L. G. Hanscom Field, Bedford, Mass.

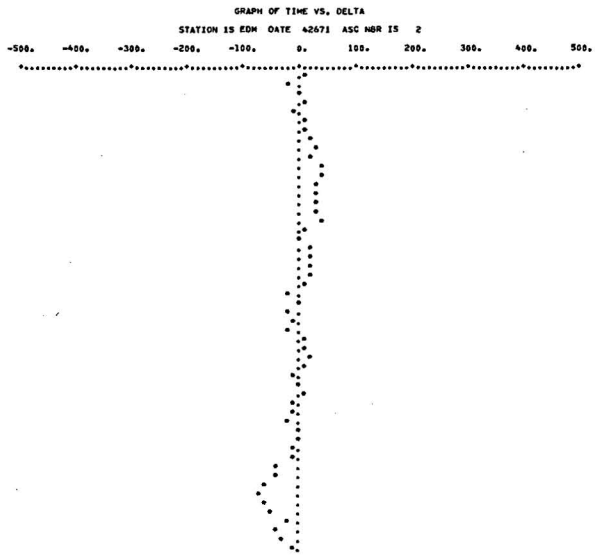

Figure A.1. Time versus delta for EDM ascent number 2.

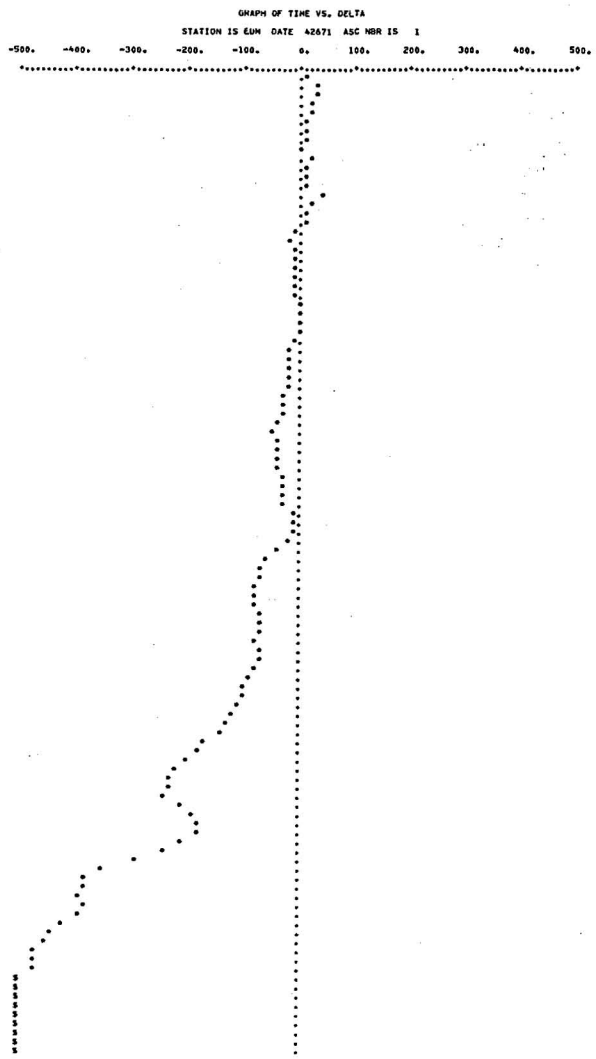

Figure A.2. Time versus delta for EDM ascent number 1.

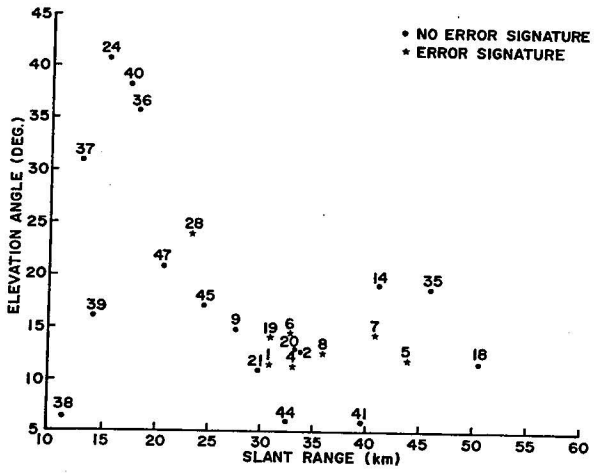

Figure A.3. Scattergram of elevation angles and slant range distances for EDM.

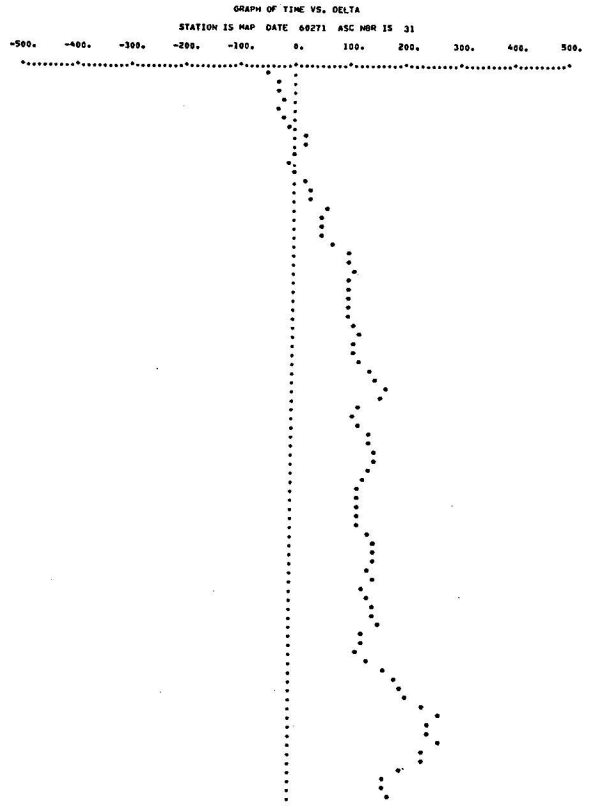

Figure A.4. Time versus delta for MAP ascent number 31.

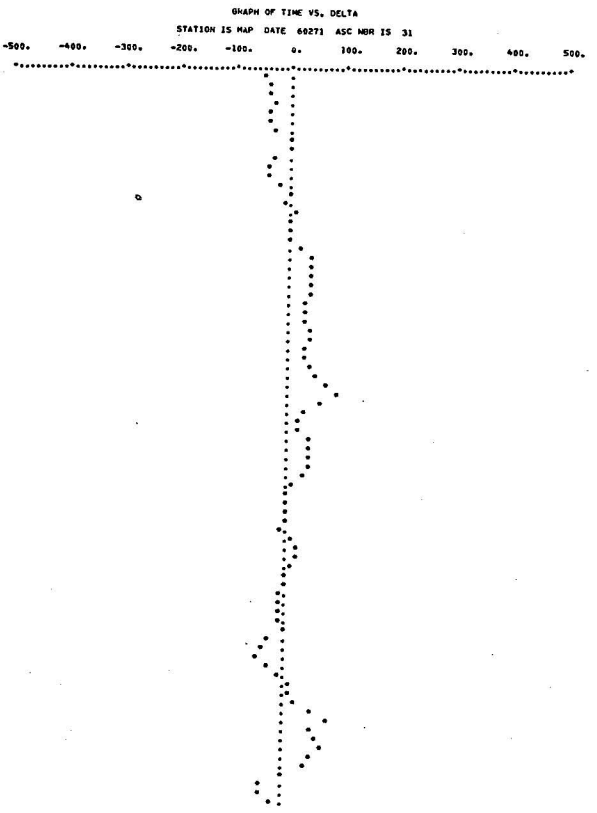

Figure A.5. Same as figure A.4 with addition of elevation angle correction.

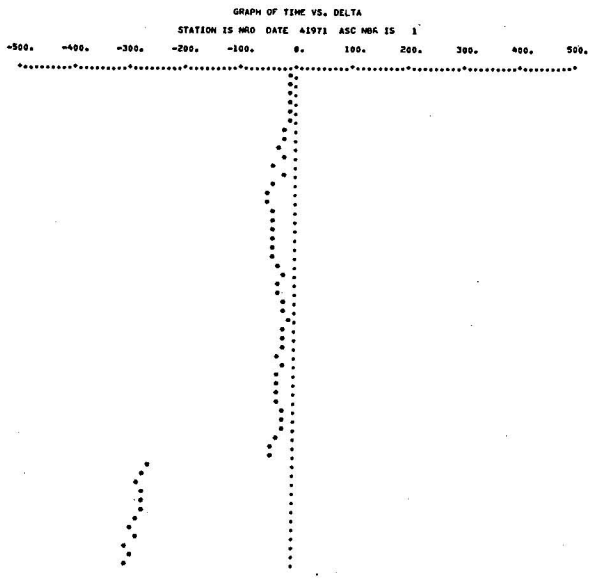

Figure A.6. Time versus delta for NRO ascent number 1.

Table A.1. Mean Absolute Delta Values (MAD) for EDM, MAP, and NRO.

EDM 1971		MAP 1971		NRO 1971	
ASC NBR	MAD [M]	ASC NBR	MAD [M]	ASC NBR	MAD [M]
1	159.5	4	404.0	1	89.1
2	23.8	5	211.2	2	27.7
4	272.2	6	161.4	3	74.5
5	192.5	7	140.7	4	805.9
6	116.9	8	239.9	5	54.4
7	71.0	9	91.1	6	135.9
8	196.5	12	163.2	7	215.7
9	21.5	13	45.5	8	125.5
13	84.8	19	46.1	9	228.4
14	38.0	20	161.7	10	171.0
18	51.8	22	49.2	11	319.7
19	164.1	23	202.5	12	337.6
20	34.1	24	35.9	15	151.0
21	41.8	28	96.2	16	148.9
24	85.4	30	177.1	17	393.9
28	39.2	31	120.6	22	132.0
35	65.3	32	187.4	23	1002.9
36	65.7	33	139.3	24	37.0
37	62.1	35	29.5	25	214.0
38	72.7	36	56.1	26	23.9
39	27.8	38	43.2	27	132.2
40	52.7	42	108.1	28	141.1
41	45.0	43	265.6	29	164.8
44	28.2	47	100.6	33	148.7
45	70.3	48	103.9	34	149.4
4	25.7			35	42.0
				36	130.3
				37	50.9
				39	19.5
				40	52.1
				41	345.0
				42	205.4
				43	41.4
				44	257.3
				45	27.1
				47	25.8
AVG.	81.1		135.2		183.9

Table A.2. Mean Absolute Delta Values (MAD) for Eight EDM Cases, Corrected and Uncorrected.

Ascension Number 1971	MAD [M]	
	No Correction	With Correction
1	159.5	20.1
4	272.2	29.0
5	192.5	63.9
6	116.9	29.0
7	71.0	38.7
8	196.5	57.9
19	164.1	30.5
28	39.2	19.0
AVG.	151.5	36.0

NATIONAL SEVERE STORMS LABORATORY

The NSSL Technical Memoranda, beginning with No. 28, continue the sequence established by the U. S. Weather Bureau National Severe Storms Project, Kansas City, Missouri. Numbers 1-22 were designated NSSP Reports. Numbers 23-27 were NSSL Reports, and 24-27 appeared as subseries of Weather Bureau Technical Notes. These reports are available from the National Technical Information Service, Operations Division, Springfield, Virginia 22151, for $3.00, and a microfiche version for $0.95. NTIS numbers are given below in parentheses.

No. 1 National Severe Storms Project Objectives and Basic Design. Staff, NSSP. March 1961. (PB-168207)

No. 2 The Development of Aircraft Investigations of Squall Lines from 1956-1960. B. B. Goddard. (PB-168208)

No. 3 Instability Lines and Their Environments as Shown by Aircraft Soundings and Quasi-Horizontal Traverses. D. T. Williams. February 1962. (PB-168209)

No. 4 On the Mechanics of the Tornado. J. R. Fulks. February 1962. (PB-168210)

No. 5 A Summary of Field Operations and Data Collection by the National Severe Storms Project in Spring 1961. J. T. Lee. March 1962. (PB-165095)

No. 6 Index to the NSSP Surface Network. T. Fujita. April 1962. (PB-168212)

No. 7 The Vertical Structure of Three Dry Lines as Revealed by Aircraft Traverses. E. L. McGuire. April 1962. (PB-168213)

No. 8 Radar Observations of a Tornado Thunderstorm in Vertical Section. Ralph J. Donaldson, Jr. April 1962. (PB-174859)

No. 9 Dynamics of Severe Convective Storms. Chester W. Newton. July 1962. (PB-163319)

No. 10 Some Measured Characteristics of Severe Storms Turbulence. Roy Steiner and Richard H. Rhyne. July 1962. (N62-16401)

No. 11 A Study of the Kinematic Properties of Certain Small-Scale Systems. D. T. Williams. October 1962. (PB-168216)

No. 12 Analysis of the Severe Weather Factor in Automatic Control of Air Route Traffic. W. Boynton Beckwith. December 1962. (PB-168217)

No. 13 500-Kc./Sec. Sferics Studies in Severe Storms. Douglas A. Kohl and John E. Miller. April 1963. (PB-168218)

No. 14 Field Operations of the National Severe Storms Project in Spring 1962. L. D. Sanders. May 1963. (PB-168219)

No. 15 Penetrations of Thunderstorms by an Aircraft Flying at Supersonic Speeds. G. P. Roys. Radar Photographs and Gust Loads in Three Storms of 1961 Rough Rider. Paul W. J. Schumacher. May 1963. (PB-168220)

No. 16 Analysis of Selected Aircraft Data from NSSP Operations, 1962. T. Fujita. May 1963. (PB-168221)

No. 17 Analysis of Methods for Small-Scale Surface Network Data. D. T. Williams. August 1963. (PB-168222)

No. 18 The Thunderstorm Wake of May 4, 1961. D. T. Williams. August 1963. (PB-168223)

No. 19 Measurements by Aircraft of Condensed Water in Great Plains Thunderstorms. George P. Roys and Edwin Kessler. July 1966. (PB-173048)

No. 20 Field Operations of the National Severe Storms Project in Spring 1963. J. T. Lee, L. D. Sanders and D. T. Williams. January 1964. (PB-168224)

No. 21 On the Motion and Predictability of Convective Systems as Related to the Upper Winds in a Case of Small Turning of Wind with Height. James C. Fankhauser. January 1964. (PB168225)

No. 22 Movement and Development Patterns of Convective Storms and Forecasting the Probability of Storm Passage at a Given Location. Chester W. Newton and James C. Fankhauser. January 1964. (PB-168226)

No. 23 Purposes and Programs of the National Severe Storms Laboratory, Norman, Oklahoma. Edwin Kessler. December 1964. (PB-166675)

No. 24 Papers on Weather Radar, Atmospheric Turbulence, Sferics, and Data Processing. August 1965. (AD-621586)

No. 25 A Comparison of Kinematically Computed Precipitation with Observed Convective Rainfall. James C. Fankhauser. September 1965. (PB-168445).

No. 26 Probing Air Motion by Doppler Analysis of Radar Clear Air Returns. Roger M. Lhermitte. May 1966. (PB-170636)

No. 27 Statistical Properties of Radar Echo Patterns and the Radar Echo Process. Larry Armijo. May 1966. The Role of the Kutta-Joukowski Force in Cloud Systems with Circulation. J. L. Goldman. May 1966. (PB-170756)

No. 28 Movement and Predictablity of Radar Echoes. James Warren Wilson. November 1966. (PB-173972)

No. 29 Notes on Thunderstorm Motions, Heights, and Circulations. T. W. Harrold, W. T. Roach, and Kenneth E. Wilk. November 1966. (AD-644899)

No. 30 Turbulence in Clear Air Near Thunderstorms. Anne Burns, Terence W. Harrold, Jack Burnham, and Clifford S. Spavins. December 1966. (PB-173992)

No. 31 Study of a Left-Moving Thunderstorm of 23 April 1964. George R. Hammond. April 1967. (PB-174681)

No. 32 Thunderstorm Circulations and Turbulence from Aircraft and Radar Data. James C. Fankhauser and J. T. Lee. April 1967. (PB-174860)

No. 33 On the Continuity of Water Substance. Edwin Kessler. April 1967. (PB-175840)

No. 34 Note on the Probing Balloon Motion by Doppler Radar. Roger M. Lhermitte. July 1967. (PB-175930)

No. 35 A Theory for the Determination of Wind and Precipitation Velocities with Doppler Radars. Larry Armijo. August 1967. (PB-176376)

No. 36 A Preliminary Evaluation of the F-100 Rough Rider Turbulence Measurement System. U. O. Lappe. October 1967. (PB-177037)

No. 37 Preliminary Quantitative Analysis of Airborne Weather Radar. Lester P. Merritt. December 1967. (PB-177188)

No. 38 On the Source of Thunderstorm Rotation. Stanley L. Barnes. March 1968. (PB-178990)

No. 39 Thunderstorm - Environment Interactions Revealed by Chaff Trajectories in the Mid-Troposphere. James C. Fankhauser. June 1968. (PB-179659)

No. 40 Objective Detection and Correction of Errors in Radiosonde Data. Rex L. Inman. June 1968. (PB-180284)

No. 41 Structure and Movement of the Severe Thunderstorms of 3 April 1964 as Revealed from Radar and Surface Mesonetwork Data Analysis. Jess Charba and Yoshikazu Sasaki. October 1968. (PB-183310)

No. 42 A Rainfall Rate Sensor. Brian E. Morgan. November 1968. (PB-183979)

No. 43 Detection and Presentation of Severe Thunderstorms by Airborne and Ground-Based Radars: A Comparative Study. Kenneth E. Wilk, John K. Carter, and J. T. Dooley. February 1969. (PB-183572)

No. 44 A Study of a Severe Local Storm of 16 April 1967. George Thomas Haglund. May 1969. (PB-184-970)

No.45 On the Relationship Between Horizontal Moisture Convergence and Convective Cloud Formation. Horace R. Hudson. March 1970. (PB-191720)

No. 46 Severe Thunderstorm Radar Echo Motion and Related Weather Events Hazardous to Aviation Operations. Peter A. Barclay and Kenneth E. Wilk. June 1970. (PB-192498)

No. 47 Evaluation of Roughness Lengths at the NSSL-WKY Meteorological Tower. Leslie D. Sanders and Allen H. Weber. August 1970. (PB-194587)

No. 48 Behavior of Winds in the Lowest 1500 ft in Central Oklahoma: June 1966 - May 1967. Kenneth C. Crawford and Horace R. Hudson. August 1970.

No. 49 Tornado Incidence Maps. Arnold Court. August 1970. (COM-71-00019)

No. 50 The Meteorologically Instrumented WKY-TV Tower Facility. John K. Carter. September 1970. (COM-71-00108)

No. 51 Papers on Operational Objective Analysis Schemes at the National Severe Storms Forecast Center. Rex L. Inman. November 1970. (COM-71-00136)

No.52 The Exploration of Certain Features of Tornado Dynamics Using a Laboratory Model. Neil B. Ward. November 1970. (COM-71-00139)

No.53 Rawinsonde Observation and Processing Techniques at the National Severe Storms Laboratory. Stanley L. Barnes, James H. Henderson and Robert J. Ketchum. April 1971.

No. 54 Model of Precipitation and Vertical Air Currents. Edwin Kessler and William C. Bumgarner. June 1971.

No. 55 The NSSL Surface Network and Observations of Hazardous Wind Gusts. Operations Staff. June 1971.

No. 56 Pilot Chaff Project at the National Severe Storms Laboratory. Edward A. Jessup. November 1971.

No. 57 Numerical Simulation of Convective Vortices. Robert P. Davies-Jones and Glenn T. Vickers. November 1971.

No. 58 The Thermal Structure of the Lowest Half Kilometer in Central Oklahoma: December 9, 1966 - May 31, 1967. R. Craig Goff and Horace R. Hudson. July 1972.

No. 59 Cloud-to-Ground Lightning Versus Radar Reflectivity in Oklahoma Thunderstorms. Gilbert D. Kinzer. September 1972.

No. 60 Simulated Real Time Displays of Velocity Fields by Doppler Radar. L. D. Hennington and G. B. Walker. November 1972.

No. 61 Gravity Current Model Applied to Analysis of Squall-Line Gust Front. Jess Charba. November 1972.

No. 62 Mesoscale Objective Map Analysis Using Weighted Time-Series Observations. Stanley L. Barnes. March 1973.

No. 63 Observations of Severe Storms on 26 and 28 April 1971. Charles L. Vlcek. April 1973.

No. 64 Meteorological Radar Signal Intensity Estimation. Dale Sirmans and R. J. Doviak. September 1973.

☆GPO 1973 — 784-569 REGION NO. 8